



Effect of microstructure evolution on mechanical properties of medium-Mn steel for hot forming

Jinbiao Wu, Cainian Jing[†], Yuhang Zhu, Qiuyue Huang, Tao Lin and Yingming Tu
School of Material science and Engineering, Shandong Jianzhu University, Jinan, 250101, China
[†]*E-mail: jcn@sdjzu.edu.cn*
www.sdjzu.edu.cn

For promoting the commercial application of third-generation advanced high-strength steels in the automotive industry, the enhancement of the mechanical properties and formability of medium-Mn steel is becoming a research hotspot. Use of self-developed hot-forming steel, the microstructure evolution on mechanical properties affected by composition and hot forming parameters of Fe-0.1C-7Mn-3Al-1.5Si medium-Mn steel was investigated in this work: analyze microstructure transformation of medium-Mn steel under hot forming process through SEM, XRD and etc.; and take the tensile strength, elongation and work hardening rate as evaluation index to study the influence on the properties of test steel such as heating process, partitioning temperature. Microstructural transformation and mechanical properties relationship are comprehensively analyzed in the test results, providing theoretical basis for optimizing the thermoforming process parameters. Achieve the goal of meeting excellent mechanical properties requirements and weight reduction of automotive components.

Keywords: Medium-Mn Steel; Hot stamping; Microstructure transformation; Automobile Lightweight.

1. Introduction

Hot forming technology for medium Mn steels has seen unprecedented growth due to its potential to produce automotive components with excellent mechanical properties and suitable cost. It can manufacture oversized and ultra-thin automotive products, and the tensile strength of the formed products can be up to 1500 MPa^[1], and the plasticity can be improved significantly (~30%) while ensuring the tensile strength. Transformation phase induced plasticity (TRIP) of residual austenite during deformation is responsible for the excellent overall mechanical properties of medium Mn steels (MMS)^[2].

The content of residual austenite and stability are the main factors influencing the TRIP effect. Studies have shown that three main factors, chemical composition content^[3], grain size^[4] and microstructural morphology^[5], influence the stability of residual austenite. In this study, Microstructure evolution effects on mechanical properties of Fe-0.1C-7Mn-3Al-1.5Si medium Mn steels was researched using a self-developed hot-forming steel. This paper analyses the factors influencing the austenite content and stability of the cold rolled medium Mn steels, as well as the influence of the TRIP effect on the deformation process in the test steels and the work-hardening behaviour.

2. Experimental materials and methods

With the aim of investigating the relationship between microstructural transformations and mechanical properties of steels after hot forming of Fe-0.1C-7Mn-3Al-1.5Si medium Mn steels, using self-developed hot-forming steel for heat treatment test. The chemical composition (wt.%) was shown in Table 1, and the measured phase transformation points A_{C1} were 674 °C and A_{C3} were 1227°C [6].

Table 1 Chemical composition of test steel (wt.%)

| Element | C | Mn | Si | Al | Cu | Mo | Cr | Nb | B | Fe |
|---------------|------|------|------|------|------|------|------|------|-------|------|
| Content/wt.-% | 0.12 | 7.69 | 1.45 | 2.76 | 0.51 | 0.20 | 0.35 | 0.11 | 0.001 | Bal. |

The cold-rolled (CR) specimens were pretreated by cyclic annealing for different times (0, 1, 2, 3, 4, 5). Among them, each cycle of annealing pretreatment includes holding at 680 °C for 10 minutes, then quenching to room temperature by water(WQ). Subsequently, a 680°C holding period of 10 minutes was performed, followed by a 150°C quench for 90 seconds in a salt bath furnace. Finally, WQ to room temperature. For convenience of description, the above specimens were numbered A0, A1, A2, A3, A4, and A5 in this paper according to the number of cycle annealing.

The heat-treated specimens were processed into standard tensile specimens of 25mm. Then use the WDW-100E type microcomputer electronic universal testing machine to stretch at 1mm/min to obtain the engineering stress-strain curve. The microstructure of the specimens was characterized using a field emission SEM (SUPRATM 55). The microstructure was characterized using a TEM (Talos F200X). Determination of the volume fraction of residual austenite using X-ray diffractometry (XRD, RIKEN Smart Lab), the scanning speed was 2°/min, the scanning range was 40°-100°. The retained austenite volume fraction is calculated using equation (1)[7]:

$$V_{\gamma} = \frac{1}{1 + \frac{I_{\alpha}K_{\gamma}}{I_{\gamma}K_{\alpha}}} \times 100\% \quad (1)$$

Where V_{γ} is the retained austenite volume fraction. I_{γ} is the combined strength of the austenite crystal diffraction peaks (200), (220) and (311). I_{α} is the combined strength of the martensite crystal diffraction peaks (200) and (211). K_{γ} and K_{α} have reflectance coefficients for austenitic and martensite phases, respectively.

The carbon content of austenite can be calculated using equation (2)[7]:

$$C_{\gamma} = (\alpha_{\gamma} - 3.547) / 0.0467 \quad (2)$$

where C_{γ} is the mass fraction of carbon in the retained austenite (%) and α_{γ} is the lattice constant of the retained austenite (220) crystal surface.

3. Results and discussion

The microstructure of each specimen that was observed by SEM was mainly martensite, austenite and ferrite as shown in Figure 1. With increasing number of cycles annealing, it

can be observed that the average size of the microstructure decreases significantly and reaches a minimum at the 4th cycle. It was analysed that the reverse-transformed austenite tends to nucleate along the more finely slatted martensite boundaries^[8], resulting in the formation of smaller sized austenite. The insufficient nucleation growth between the phases is responsible for the decrease in grain size with numbers of annealing. However, as the number of annealing increases, smaller austenite grains occur grain consolidation during the annealing process and the phase size shows an increasing trend, as shown in Figure 1(f).

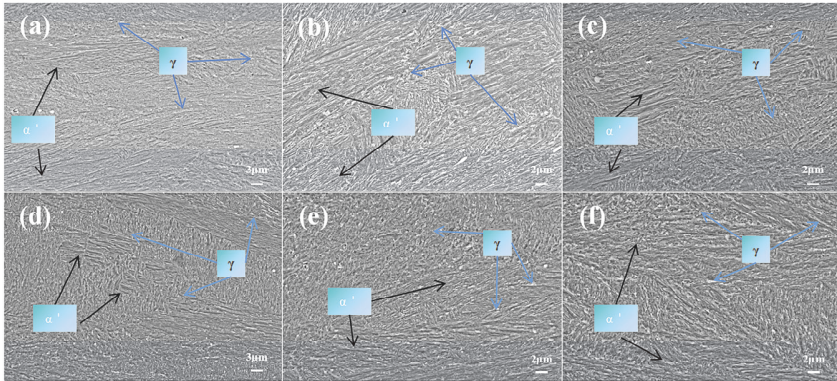


Figure 1. (a), (b), (c), (d), (e), (f) SEM images of test steels A0, A1, A2, A3, A4, A5, respectively.

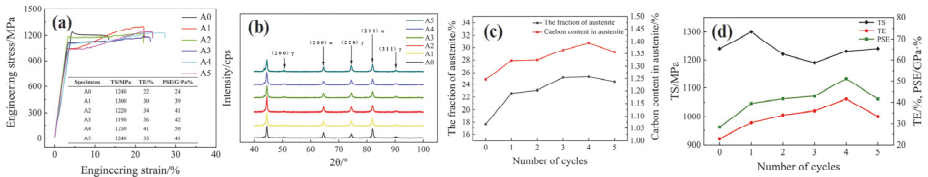


Figure 2. Test data of different pre-cycle annealing test steels: (a) engineering strain-strain curves, (b) XRD diffraction peak images, (c) Residual austenite volume fraction and the carbon content in residual austenite images, and (d) mechanical properties.

Engineering stress-strain curves of test steels under different heat treatment processes are shown in Figure 2(a). In particular, the best overall mechanical properties are the product of strength and elongation of A4 samples up to 51 GPa·%, with a tensile strength of 1230 MPa and an elongation of 41%. It can be found that a sparse sawtooth pattern is present on engineering stress-strain curves, indicating discontinuous yielding during deformation. In addition to the discontinuous TRIP effect^[9], which causes this phenomenon, it can also be caused by dynamic ageing^[10]. Significant increase in elongation and PSE of test steels with increasing number of annealing cycles as shown in Figure 2. (d). Residual austenite content and carbon content in residual austenite also trending upwards. Among them, the highest residual austenite content and the highest carbon content in residual austenite were found in the A4 specimen, which resulted in the best comprehensive mechanical properties. It was analyzed that, on the one hand, the austenite grain size of the A4 specimens was significantly reduced, and the surface area of the interface between the austenite grains and the surrounding phases was increased after

cyclic annealing. The larger phase interface area allows more channels for austenitic grains to absorb C atoms from neighboring grains, so finer austenitic grains have higher C content, which improves austenitic stability.

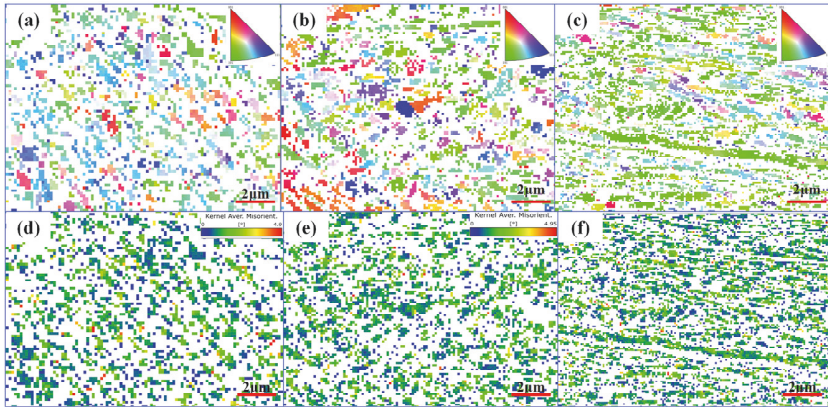


Figure 3. IPF (a, b, c) and KAM maps (d, e, f) for test steels A0, A1 and A4.

After several cycles of quenching, the differences in grain orientation become smaller. The more uniform grain orientation contributes to the deformation co-ordination between the tissues of the material during the deformation process [7]. Therefore, pre-treatment of cold rolled steel improves the coordination of deformation in the microstructure of the material after hot stamping. From the comparative analysis of the EBSD data, it was found that there was not much difference in the KAM values in the BCC phase, which is possibly due to the reversion and recrystallisation of the microstructure occurred at the Q&P process annealing stage [11,12]. Therefore, materials plastic deformation processes are not only affected by grain size, the grain orientation in the microstructure is also affected.

4. Conclusions

(1) Pre-treatment with cyclic annealing can significantly improve the mechanical properties of the medium Mn Q&P steel, with a tensile strength of 1230 MPa, an elongation of 41%, and a product of strength and elongation of 50 GPa·% for the A4 specimen.

(2) Pre-treatment with cyclic annealing improves the content of elemental C in the residual austenite and obtains a moderately stable residual austenite. The RA content of the A4 specimen reaches 25%, while the C content in RA also reaches a maximum of 1%.

(3) The pre-treatment with cyclic annealing resulted in a more uniform grain orientation, improved homogeneous deformation of the test steel, and a more sustained TRIP effect, which greatly improved the comprehensive mechanical properties.

References

1. X. L. Zhao, Y. J. Zhang, C. Y. Wang and HUI Weijun, Effect of heating temperature on the hydrogen embrittlement susceptibility in hot stamped medium-Mn steel. *Chin J Mech Eng-En.* 5853-862(2024).

2. Cai, Z.H., Ding, H., Kamoutsi, H., Haidemenopoulos, G.N., Misra, R.D.K.: Interplay between deformation behavior and mechanical properties of intercritically annealed and tempered medium-manganese transformation-induced plasticity steel. *Mat Sci Eng A-Struct.* 654, 359–367 (2016).
3. Li, J., Song, R., Li, X., Zhou, N., Song, R.: Microstructural evolution and tensile properties of 70 GPa-% grade strong and ductile hot-rolled 6Mn steel treated by intercritical annealing. *Mat Sci Eng A-Struct.* 745, 212–220 (2019).
4. Hanzaki, A.Z., Hodgson, P.D., Yue, S.: Retained austenite characteristics in thermomechanically processed Si-Mn transformation-induced plasticity steels. *Metall Mater Trans A.* 2405–2414 (1997).
5. Misra, R.D.K., Venkatsurya, P., Wu, K.M., Karjalainen, L.P.: Ultrahigh strength martensite–austenite dual-phase steels with ultrafine structure: The response to indentation experiments. *Mat Sci Eng A-Struct.* 560, 693–699 (2013).
6. Feng, Y., Jing, C., Lin, T., Wu, Z., Li, Z., Zhao, J.: Effect of retained austenite on the microstructure and mechanical properties of cold-rolled medium-manganese Q&P steel. *Ironmak Steelmak.* 167–173 (2023).
7. Wu, Z., Jing, C., Feng, Y., Li, Z., Lin, T., Zhao, J., Liu, L.: Effect of a new pretreatment-Q&P process on the microstructure and mechanical properties of light-weight Al-containing medium-Mn steels. *Mat Sci Eng A-Struct.* 144468 (2023).
8. Zhang, L., Huang, X., Wang, Y., Guo, Y., Dai, G., Li, D.: Achieving Excellent Strength–Ductility and Impact Toughness Combination by Cyclic Quenching in Medium Mn TRIP-Aided Steel. *J Mater Eng Perform.* 27, 5769–5777 (2018).
9. Santofimia, M.J., Zhao, L., Petrov, R., Kwakernaak, C., Sloof, W.G., Sietsma, J.: Microstructural development during the quenching and partitioning process in a newly designed low-carbon steel. *Acta Mater.* 59, 6059–6068 (2011).
10. Lu, J., Yu, H., Kang, P., Duan, X., Song, C.: Study of microstructure, mechanical properties and impact-abrasive wear behavior of medium-carbon steel treated by quenching and partitioning (Q&P) process. *Wear.* 414–415, 21–30 (2018).
11. Li, Z.C., Misra, R.D.K., Cai, Z.H., Li, H.X., Ding, H.: Mechanical properties and deformation behavior in hot-rolled 0.2C-1.5/3Al-8.5Mn-Fe TRIP steel: The discontinuous TRIP effect. *Mat Sci Eng A-Struct.* 63–72 (2016).
12. Benzing, J.T., Kwiatkowski da Silva, A., Morsdorf, L., Bentley, J., Ponge, D., Dutta, A., Han, J., McBride, J.R., Van Leer, B., Gault, B., Raabe, D., Wittig, J.E.: Multi-scale characterization of austenite reversion and martensite recovery in a cold-rolled medium-Mn steel. *Acta Mater.* 166, 512–530 (2019).

Open Access This chapter is licensed under the terms of the Creative Commons Attribution-NonCommercial 4.0 International License (<http://creativecommons.org/licenses/by-nc/4.0/>), which permits any noncommercial use, sharing, adaptation, distribution and reproduction in any medium or format, as long as you give appropriate credit to the original author(s) and the source, provide a link to the Creative Commons license and indicate if changes were made.

The images or other third party material in this chapter are included in the chapter's Creative Commons license, unless indicated otherwise in a credit line to the material. If material is not included in the chapter's Creative Commons license and your intended use is not permitted by statutory regulation or exceeds the permitted use, you will need to obtain permission directly from the copyright holder.

